Pergamon

PII: S0191-8141(96)00091-0

Journal of Structural Geology, Vol. 19, Nos 3–4, pp. 249 to 256, 1997

0191-8141/97 $17.00+0.00

Fault-propagation, ductile strain, and displacement–distance relationships

CHRISTOPHER A. HEDLUND*

Department of Earth Resources, Colorado State University, Fort Collins, CO 80523, U.S.A.

(*Received* 2 *February* 1996; *accepted in revised form* 8 *October* 1996)

Abstract—Displacement–distance analysis of fault-related fold structures can reveal important information about the distribution of fault displacement, and, in some cases, the history of fault propagation. This method is commonly used to: (1) determine the ratio of displacement rate to propagation rate (s/p ratio), (2) predict the location of unconstrained fault tips, (3) determine the location of fault nucleation points, and (4) evaluate structural interpretations. Although the displacement–distance approach represents a potentially useful method for gaining information about displacement-parallel fault propagation histories of natural fault-related fold structures, the theoretical relationship between s/p and relative stretch (ε_r) that forms the basis of this method remains essentially untested. Because displacement rates and propagation rates are generally unknown for natural structures, these relationships can only be objectively tested by analysing model structures with known geometries, strain distributions, and fault propagation histories. Displacement–distance analysis of different fault-related fold models reveals that: (1) displacement–distance relationships are highly dependent on the nature of the hanging wall strain, (2) relative stretch is not related to s/p in any general way, (3) fault tip locations cannot always be predicted by linear extrapolation of displacement–distance trajectories, (4) displacement maxima are not necessarily indicative of fault nucleation points in all cases, and (5) although calculation of s/p ratios from observed relative stretch magnitudes may not be appropriate, the use of displacement–distance relationships can nonetheless be useful in comparing structures and improving structural interpretations.

INTRODUCTION

The question of how faults initiate and propagate is of fundamental importance to the evolution and interpretation of fold–thrust structures. Because the processes of fault nucleation, propagation, and displacement cannot generally be observed directly in natural structures, various theoretical approaches have been used to evaluate and predict the relative importance and rates of these processes. Williams and Chapman (1983) introduced displacement–distance analysis as a method for characterizing the distribution of displacement and for interpreting the propagation histories of natural faults. Displacement–distance analysis is commonly used to determine the ratio of fault slip (displacement) to propagation, or s/p ratio (Williams and Chapman, 1983; Chapman and Williams, 1984; Dominic and McConnell, 1994), predict the location of unconstrained fault tips (Williams and Chapman, 1983; Chapman and Williams, 1984), determine the location of fault nucleation points (Ellis and Dunlap, 1988; Kattenhorn and McConnell, 1993), and evaluate structural interpretations (McConnell, 1994).

Although the displacement–distance approach represents a potentially useful method for gaining information about fault propagation histories of natural structures, the theoretical relationship between s/p and relative stretch (ε_r) that forms the basis of this method remains essentially untested. Because displacement and propagation histories are generally unknown for natural structures, these relationships can only be objectively tested by analysing model structures with known geometries, strain distributions, and fault propagation histories. This paper presents results from displacement–distance analysis of several different fault-related fold models with known geometries, strain distributions, and fault propagation histories, and discusses the results of these analyses for the interpretation of propagation histories for natural faults based on displacement–distance relationships.

Displacement–distance relationships

Williams and Chapman (1983) realized the interdependency of fault propagation, displacement, and internal strain within a thrust sheet, and proposed a dislocation analogy for propagating faults where displacement decreases toward the fault tip in the direction of transport (Fig. 1a & b). The variation in displacement along the fault can be illustrated on a displacement–distance plot (Fig. 1c), where the cutoff separation (displacement) is plotted as a function of position measured along the fault relative to an arbitrary reference point (Williams and Chapman, 1983).

In the Williams and Chapman (1983) dislocation model, hanging wall strain occurs by homogeneous pure shear with a greatest shortening axis parallel to a planar fault (fault-parallel pure shear; Fig. 1). Based on this model, Williams and Chapman (1983) derived a quantitative relationship between relative stretch (ε_r), and ratio of the slip to propagation (s/p) such that

*Present address: Shell E & P Technology Co., P.O. Box 481, Houston, TX 77001-0481, U.S.A.

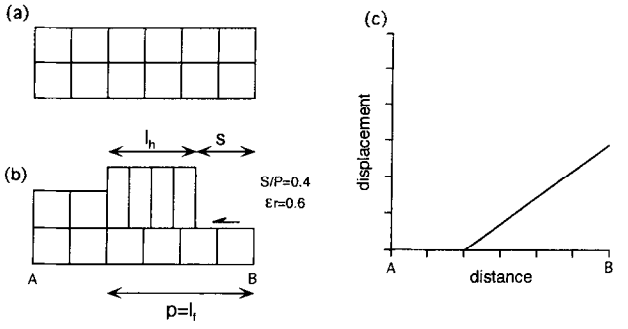

Fig. 1. Williams and Chapman (1983) dislocation model used in the derivation of the relationship between ε_r and s/p ratio in equation (1). (a) Model before displacement. (b) Model with 40% hanging wall shortening by fault-parallel pure shear and associated propagation of the planar fault. (c) Displacement–distance plot corresponding to (b). Vertical and horizontal scales are identical. Points A & B in (c) correspond to A & B in (b). Figure modified after Williams and Chapman (1983).

$$\varepsilon_r = 1 - \frac{s}{p}, \tag{1}$$

where s is the fault slip (displacement) and p is the propagated fault length. For contractional structures, the relative stretch measured parallel to the fault is given by

$$\varepsilon_r = \frac{l_h}{l_f}, \tag{2}$$

where l_f is the initial, or footwall cutoff length, and l_h is the deformed, or hanging wall cutoff length.

Fault-parallel pure shear of the type assumed in the Williams and Chapman (1983) model is widely recognized in foreland fold–thrust belts (i.e. layer-parallel shortening of Geiser and Engelder, 1983; Geiser, 1988), but it represents only one of the possible end-member types of strain in thrust sheets (Coward and Kim, 1981; Sanderson, 1982). Bedding-parallel simple shear (flexural flow or flexural slip) is also widely recognized in fold–thrust belts, and is interpreted to be an important mechanism in many structures characterized by parallel folding (Chapple and Spang, 1974, among others). Bedding-parallel simple shear will generally result in changes in bed-cutoff lengths (Suppe, 1983; DePaor, 1987; Ferrill, 1988; Rowan and Ratliff, 1988) and associated transport-parallel displacement gradients along the fault.

In addition to determining s/p ratios, displacement–distance methods have been used to estimate the positions of fault tips and nucleation points, and to improve structural interpretations. Williams and Chapman (1983) and Chapman and Williams (1984) project displacement–distance trajectories towards the axis where displacement = 0 to estimate the position of the fault tip. Assuming that displacement is time-dependent such that the oldest fault segments will have the greatest displacement, displacement maxima on a displacement–distance plot are often taken to represent the nucleation point of the fault (Ellis and Dunlap, 1988; Kattenhorn and McConnell, 1993). A more subjective use of displacement–distance diagrams involves the use of these plots in evaluating and improving structural interpretations (McConnell, 1994).

Displacement–distance analysis of fault-related fold models

It is generally not possible to evaluate the relationships between fault propagation, ductile strain, and displacement–distance relationships of natural structures because fault propagation histories for natural structures are generally not known, and because representative structures with well-exposed cutoff geometries and known strain distributions are rare. For this reason, fault-related fold models with known fault propagation histories, cutoff geometries, and strain distributions are used in this study to evaluate the predictions of Williams and Chapman's (1983) theoretical relationship between s/p and ε_r. Models analysed in this study include the fault-propagation fold models of Suppe and Medwedeff (1984, 1990), Jamison (1987), Chester and Chester (1990), Mitra (1990), and Erslev (1991), the paper card ramp-fold model of Elliott (1976), the fault-bend fold model of Suppe (1983), a fault-bend fold model with a curved ramp geometry and a generalized décollement fold model. All of the models are characterized by bedding-parallel simple shear deformation, and the décollement fold model also features heterogeneous ductile shear in the décollement zone. The geometries, kinematics, and strain distributions of these models are well constrained. In all cases, the models analysed in this study either originate with a pre-existing fault (i.e. $s/p = 0$), or propagate from a known point and at a known rate.

These models are certainly not representative of natural structures in all respects, but they do incorporate strain mechanisms (i.e. bedding-parallel simple shear) and geometries that are reasonable to the first approximation, and thus represent possible end-member processes in nature. Thus these models can be used to illustrate some of the important relationships between fault propagation, ductile strain, and displacement–distance relationships that may be analogous to natural structures. Furthermore, if the displacement–distance relationships outlined by Williams and Chapman (1983) are generally applicable to the heterogeneous and complex strain distributions in all natural structures, they should also be appropriate for the analysis of these relatively simple model structures.

Fault-propagation folds

Fault-propagation folds form due to shortening in front of a propagating fault tip (Suppe and Medwedeff, 1984, 1990). The original fault-propagation fold model (Fig. 2a) involves angular/kink folding at axial surfaces fixed with respect to a uniformly dipping thrust ramp propagating upwards from an existing flat (Suppe and Medwedeff, 1984, 1990). In addition to the imposed

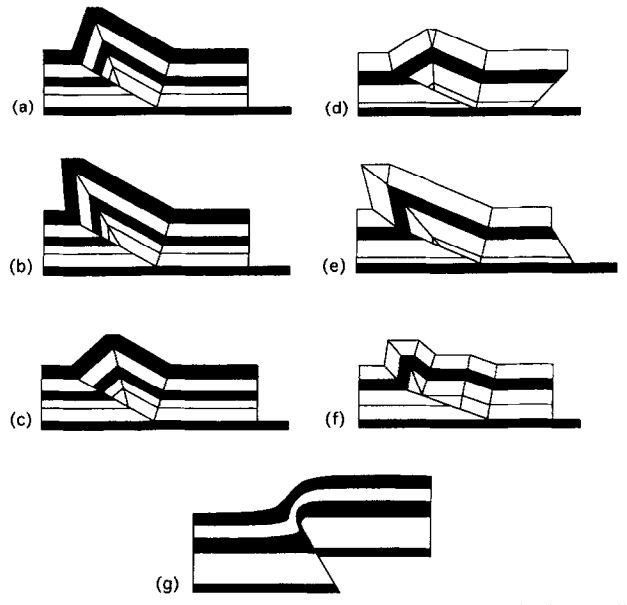

Fig. 2. Fault-propagation fold models analysed in this study. (a) Parallel fault-propagation fold (modified after Suppe and Medwedeff, 1984, 1990). (b) Fault-propagation fold with 25% forelimb thinning (modified after Jamison, 1987). (c) Fault-propagation fold with 25% forelimb thickening (modified after Jamison, 1987). (d) Fault-propagation fold with antithetic (top-to-the-hinterland) bedding-parallel simple shear at trailing edge loose line (modified after Mitra, 1990). (e) Fault-propagation fold with synthetic (top-to-the-foreland) bedding-parallel simple shear at trailing edge loose line (modified after Mitra, 1990). (f) Fault-propagation fold developed over a thrust with constant dip (modified after Chester and Chester, 1990). (g) Trishear fault-propagation fold (Erslev, 1991).

geometric boundary conditions of the fault, this model assumes deformation by distributed bedding-parallel shear, or flexural flow, resulting in a parallel fold geometry and conservation of bed length (Suppe and Medwedeff, 1984, 1990). Displacement–distance analysis of this fault-propagation fold model (Fig. 3) reveals a constant displacement segment corresponding to the hanging wall flat (horizontal trajectory on displacement–distance plot), and a segment with a linear displacement gradient sloping down from the maximum displacement to zero at the fault tip (corresponding to the hanging wall ramp). The s/p ratio calculated from the measured relative stretch value using equation (1) agrees with the actual s/p ratio. The relationship between s/p ratio and relative stretch for the Suppe and Medwedeff (1984, 1990) fault-propagation fold model (equation A5) is identical to that derived for the Williams and Chapman (1983) dislocation model (equation 1), despite the fact that the fault geometry (ramp-flat vs planar) and strain mechanisms (bedding-parallel simple shear vs fault-parallel pure shear) are completely different in the two models (see Appendix). This suggests that equation (1) accurately describes the relationship between relative stretch and s/p ratio for any general fault-propagation fold model characterized by a linear displacement gradient and a propagation rate higher than the displacement rate (i.e. $0<s/p<1$). The actual values of relative stretch and s/p ratio for a fault-propagation fold are dependant on the dip of the thrust ramp. Figure 4 shows how relative stretch increases with increasing dip for the Suppe and Medwedeff (1984, 1990) fault-propagation fold model.

Since the introduction of the original fault-propagation fold model by Suppe and Medwedeff (1984), several modifications have been added. Jamison (1987) modified Suppe and Medwedeff's (1984) model to include a component of forelimb thinning (Fig. 2b) or thickening (Fig. 2c). Mitra (1990) considered the case where additional synthetic (top-to-the-foreland) or antithetic (top-to-the-hinterland) bedding-parallel simple shear was added to the fault-propagation fold, resulting in an inclined trailing edge loose line (Fig. 3d & e). Chester and Chester (1990) adapted the fault-propagation fold model to the case where the fold forms above a planar thrust (Fig. 2f). Each of these modified fault-propagation fold models yield displacement–distance plots similar to the original model (Fig. 3), although the exact relationship between relative stretch and s/p ratio is different.

Trishear fault-propagation folding (Erslev, 1991) represents another end-member fault-propagation fold model where displacement is transferred from a discrete

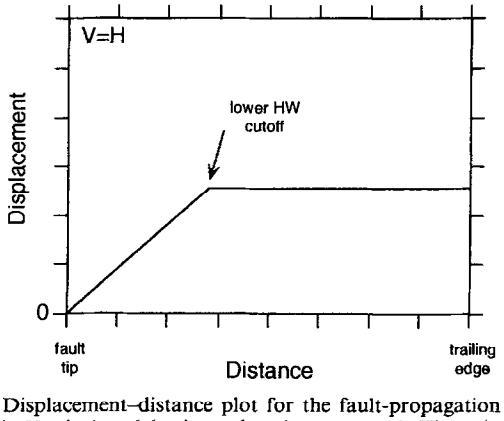

Fig. 3. Displacement–distance plot for the fault-propagation fold in Fig. 2(a). Vertical and horizontal scales are equal. The other fault-propagation fold models considered in this study yield similar displacement–distance trajectories, although the displacement gradient and relative stretch may be different for a given ramp angle.

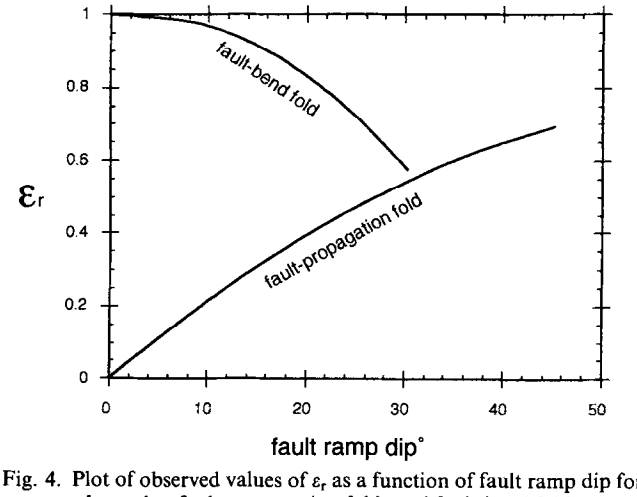

Fig. 4. Plot of observed values of ε_r as a function of fault ramp dip for end-member fault-propagation folds and fault-bend folds.

fault at depth to a broader, triangular-shaped shear zone at higher structural levels (i.e. shear strain decreases as the shear zone widens). Displacement–distance analysis of trishear fault-propagation folds reveals a constant displacement segment (below the intital tip position) and a linear displacement gradient segment (above the initial tip position), similar to other fault-propagation fold models.

Fault-bend folds

Rich (1934) recognized that folds can form in response to displacement on a non-planar fault surface. This process, known as fault-bend folding, has been subsequently studied in detail and quantified by Suppe (1983). The Suppe (1983) fault-bend fold model assumes that the fault exists at the earliest stages of displacement (i.e. the propagation rate is instantaneous relative to the displacement rate, so $s/p=0$). Although this assumption is obviously not valid in all cases, it may be reasonable for many structures. The fault-bend fold model provides an explanation for strain that is unrelated to thrust tip propagation.

Elliott (1976) produced a physical analog fault-bend fold model by shearing a stack of paper computer cards above a precut, curved fault surface (Fig. 5a). Because of the layer-parallel anisotropy of the cards, deformation in the model occurred by bedding-parallel simple shear. Additional top-to-the-foreland shear unrelated to folding results in an inclined trailing edge loose line, and increased displacement in the direction of transport at the leading edge of the structure. A displacement–distance plot for this structure (Fig. 6a) reveals that the displacement along the fault increases in the direction of transport, with the displacement gradient occurring along the hanging wall ramp. This is consistent with cutoff length modification by layer-parallel simple shear.

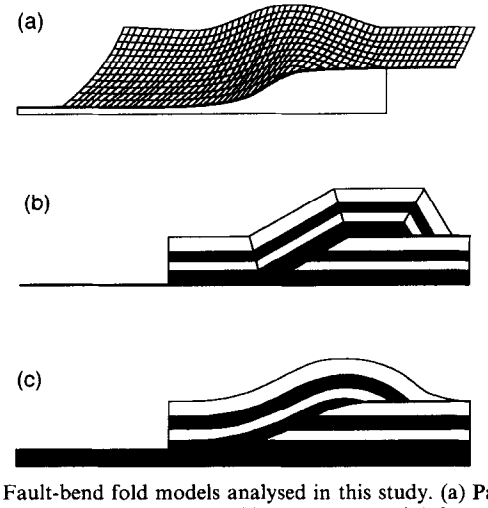

Fig. 5. Fault-bend fold models analysed in this study. (a) Paper card ramp fold model (modified after Elliott, 1976). (b) Kink fault-bend fold developed over a planar ramp (modified after Suppe, 1983). (c) Fault-bend fold developed over a curved ramp (forward modeled using GEOSEC^{TM}).

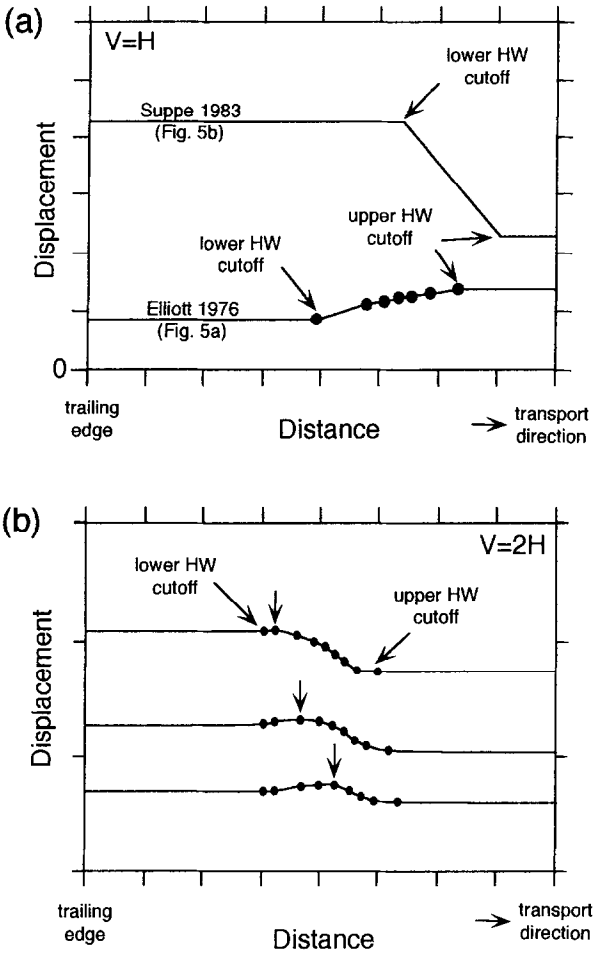

Fig. 6. (a) Displacement–distance plots for the fault-bend fold models in Fig. 5(a) and (b). Vertical and horizontal scales are equal. (b) Displacement–distance plots for three stages of displacement of the fault-bend fold model in Fig. 5(c) (c represents the maximum displacement). Vertical exaggeration = 2×. Distance is measured relative to the trailing edge of the hanging wall in each case. Vertical arrows indicate the location of the displacement maximum.

Despite the fact that $s/p=0$, the layer-parallel simple shear results in a finite relative stretch. Thus the relationship between s/p and relative stretch in this model cannot be explained by equation (1).

A simple fault-bend fold model with a planar ramp and angular fault bends is shown in Fig. 5(b) (modified after Suppe, 1983). Deformation in this model also occurs by layer-parallel simple shear, resulting in a parallel fold geometry. Displacement–distance analysis of this structure results in a stepped displacement–distance trajectory (Fig. 6a), with constant displacement along the hanging wall flat and a linear decrease in displacement (constant relative stretch and displacement gradient) along the hanging wall ramp. As with the Elliott (1976) model, this is consistent with the bedding-parallel simple shear deformation. Because no additional trailing-edge shear was included in this model, and because of the sense and magnitude of simple shear in the forelimb, the hanging wall cutoff lengths decrease in length in this model. This distribution of shear results in a displacement decrease in the direction of transport. Like the fault-propagation

fold model, the magnitude of relative stretch in the fault-bend fold model depends on the ramp dip (Fig. 4). As with the Elliott (1976) model, the relationship between s/p (0) and relative stretch (finite value) in this model cannot be explained by equation (1).

Figure 5(c) shows a forward model of a fault-bend fold formed above a curved ramp (actually approximated by many linear segments). This model was created using GEOSEC^{TM}, a computer program which uses a flexural (bedding-parallel) simple shear algorithm to forward model fault-bend folds (Geiser *et al.*, 1988). Figure 6(b) shows displacement–distance plots for three different stages of displacement of this structure (Fig. 5c illustrates the final stage of displacement). The three plots are displayed with distance measured relative to the trailing edge of the hanging wall (left side of plot), and the vertical arrows indicate the maximum displacement on each of the curves. In each case, the maximum displacement occurs somewhere over the ramp. This distribution of displacement maxima can be explained in terms of the distribution of simple shear in the structure. Where hanging wall cutoffs are juxtaposed against steeper footwall cutoffs, synthetic simple shear in the hanging wall lengthens the cutoffs, and where hanging wall cutoffs are juxtaposed against shallower footwall cutoffs, antithetic simple shear in the hanging wall shortens the cutoffs. As displacement increases, the position of the displacement maximum migrates towards the lower hanging wall cutoff. Eventually, when the lower hanging wall cutoff reaches the upper footwall cutoff, the displacement maximum will coincide with the lower hanging wall flat. A fault-bend fold modeled on a similar ramp but with a vertical simple shear deformation mechanism results in a similar distribution of displacement.

Figure 7 shows a plot of measured values of relative stretch (and calculated values of s/p) for three bed cutoff segments originating from the lower and middle parts of the ramp with cutoff angles of 15°, 20°, and 30°. This plot indicates that bed cutoff lengths, and thus values of relative stretch, change with increasing displacement in response to fault-bend folding by simple shear. The 15° and 20° cutoff segments first increase in length (relative stretch > 1), and then decrease in length (relative stretch < 1) as they are translated over steeper, and then shallower parts of the footwall ramp. The 30° cutoff segment originates at the steepest part of the ramp and thus only decreases in length with translation over the shallower dipping upper parts of the footwall ramp. Because the magnitude, and potentially the sense, of simple shear changes, cutoff lengths and relative stretch magnitudes change as well. In this case, the relative stretch is unrelated to the process of fault propagation, and only reflects hanging wall strain associated with translation over the curved fault surface (i.e. fault-bend folding). Because the value of relative stretch for each cutoff segment changes with increased displacement, the value of the s/p ratio calculated from equation (1) also changes. If the calculated s/p ratio is reflective of the actual rates of displacement and propagation, it would not be expected to change with displacement. Furthermore, the actual s/p ratio is equal to 0 in this model despite the finite relative stretch values. Thus equation (1) does not satisfactorily describe the relationship between s/p and relative stretch in this model.

Décollement folds

Décollement, or detachment folds form by displacement and differential shortening of the hanging wall above a bedding-parallel fault, or décollement zone, which may occur either at a fault tip or within a thrust sheet (Jamison, 1987; Mitra and Namson, 1989). Unlike the case for fault-propagation folds, differential shortening is independent of fault propagation in décollement folds, and can be accommodated above a fault that is propagating faster than the displacement rate ($s/p < 1$), propagating slower than the displacement rate ($s/p > 1$), or not propagating ($s/p = \infty$). For example, décollement folds may develop at a discontinuity on a décollement (i.e. high-angle fault offset) or at a stratigraphic pinchout of a décollement zone (Goguel, 1962, p. 164; Laubscher, 1977), thus allowing displacement to accumulate without propagation of the fault tip.

Because of the wide range of possible décollement fold geometries, no simple geometric/kinematic model for décollement folding exists (Homza and Wallace, 1995). It is useful, however, to consider the implications of décollement fold evolution in certain conditions possible in nature, specifically the case where a fold forms above a non-propagating fault. Figure 8 shows the evolution of an area-balanced décollement fold forming above a non-propagating décollement surface. Bed length and thickness is conserved in the upper layers, as is consistent with deformation by bedding-parallel simple shear. Deformation in the décollement zone, however, is heterogeneous. Although the exact displacement–distance relationships cannot be determined because of the lack of bed cutoffs in the heterogeneously sheared décollement zone, a displacement–distance plot for this model will be similar to that for the fault propagation fold (Fig. 3), where displacement is constant along the flat behind the fold, and decreases to zero at the fault tip. The displacement gradient near the fault tip results in a finite relative stretch, yet $s/p = \infty$ for this model. Thus equation (1) will not accurately describe the relationship between s/p and relative stretch for décollement folds in general.

DISCUSSION

Figure 9 shows a plot of the observed values of relative stretch (ε_r) plotted as a function of s/p for the model structures analysed in this study. The relationship (Williams and Chapman, 1983) between ε_r and s/p, equation (1), is also plotted for reference. As suggested

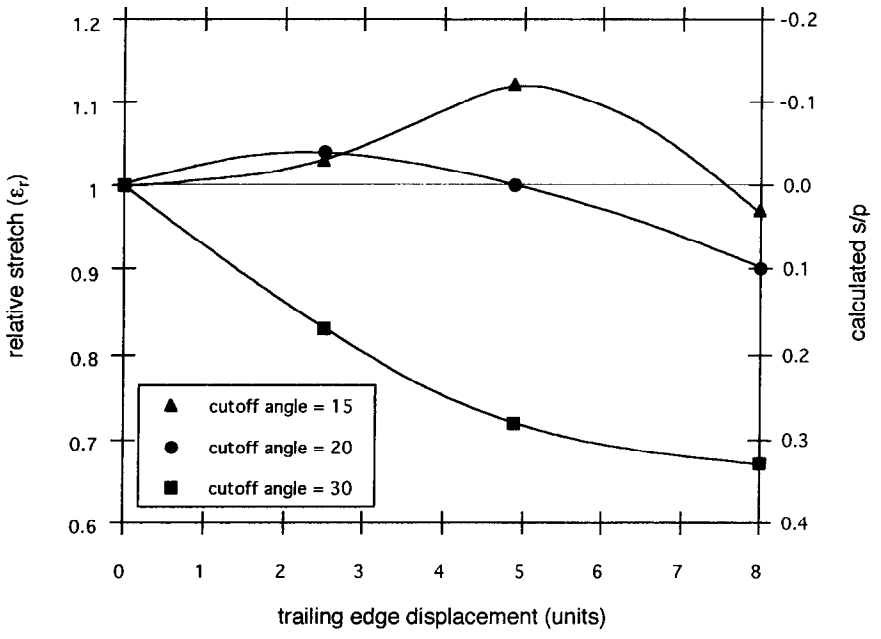

Fig. 7. Plot of measured ε_r and calculated s/p as a function of displacement for three hanging wall cutoff segments in the fault-bend fold of Fig. 6(c). Cutoff segments correspond to the 15°, 20°, and 30° cutoffs from the lower and middle part of the ramp. See text for discussion.

in the previous section, the empirical data determined from the model structures do not always coincide with the Williams and Chapman (1983) relationship (equation 1). Fault propagation folds follow the Williams and Chapman (1983) relationship. Fault-bend folds plot along the $s/p=0$ axis, and may have relative stretch values of $0<s/p<1$ (displacement decreases in the direction of transport) or $s/p>1$ (displacement increases in the direction of transport). Décollement folds have a wide range of possible positions, and s/p values may range up to infinity. Observed values of relative stretch range from 0 to >1, and observed values of s/p range from 0 (fault-bend folds) to infinity (non-propagating décollement folds). The observed ranges of both of these parameters are outside of the range of possible values predicted by equation (1), given the constraints of $s/p\geq 0$ and $\varepsilon_r\geq 0$ (cutoff lengths cannot be less than 0). The observed pattern suggests a wide range of possible relationships between relative stretch and s/p. Thus calculation of s/p ratios from measured values of relative stretch using equation (1) may result in inaccurate s/p ratios.

The use of displacement–distance plots in predicting fault tip locations is successful in cases where displacement gradients are linear and displacement decreases in the direction of transport (i.e. fault-propagation fold

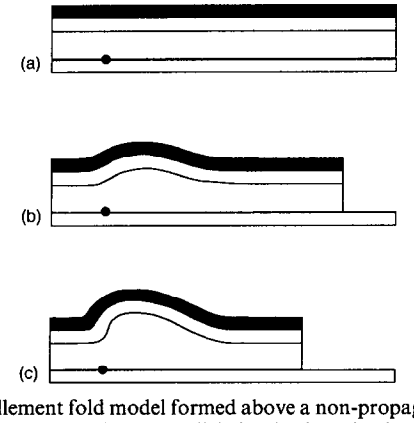

Fig. 8. Décollement fold model formed above a non-propagating fault. Deformation occurs by layer-parallel simple shear in the upper beds, and by heterogeneous shear in the décollement zone. Circle represents fault tip position.

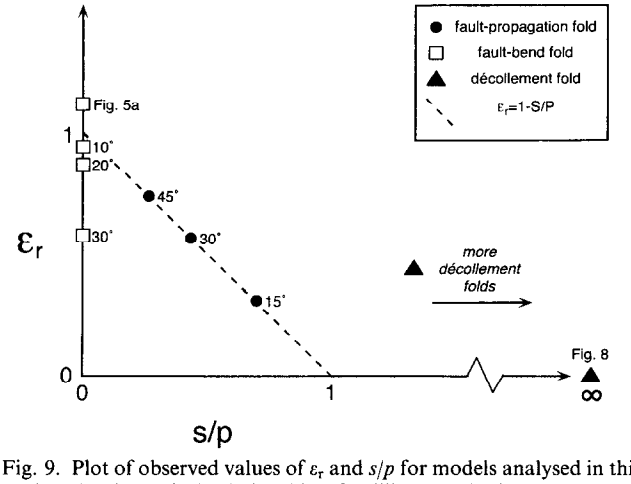

Fig. 9. Plot of observed values of ε_r and s/p for models analysed in this study. The theoretical relationship of Williams and Chapman (1983), equation (1), is plotted for reference. Numbers adjacent to data represent ramp angles. Data for Figs 5(a) and 8 as labeled. See text for discussion.

models). Where displacement gradients are unrelated to fault propagation (i.e. fault-bend fold models), or where displacement increases in the direction of transport (i.e. Elliott (1976) model), however, extrapolation from displacement–distance relationships will give a false tip location.

Displacement maxima on displacement–distance plots are often taken to represent fault nucleation points. Strain due to simple shear unrelated to fault propagation, however, may result in displacement maxima that are not coincident with fault nucleation points. For example, despite the fact that the the fault in the fault-bend fold model in Fig. 5(c) originated before any displacement occurred ($s/p = 0$), layer-parallel simple shear in response to translation over the footwall ramp resulted in a local displacement maxima (Fig. 6b).

Although the relationship between s/p and ε_r given in equation (1) may not be generally valid for all fold–thrust structures, many of the conclusions based on s/p ratios determined from equation (1) are nonetheless good. For example, although the s/p ratios determined using this relationship may not be exactly correct, comparison of s/p ratios in a qualitative way can lead to an improved interpretation (Dominic and McConnell, 1994). Similarly, the nucleation points determined by Ellis and Dunlap (1988) are reasonable given the fact that the fault tip line often intersects the plane of section at both ends, and the faults are nearly planar in section. Displacement distance analysis can also be used to recognize the presence of branch lines, which may appear as displacement discontinuities or jogs on displacement–distance diagrams (Williams and Chapman, 1983). These approaches can be useful in evaluating and improving structural interpretations where other constraints are not available. In addition, the relationships between relative stretch magnitudes and fault cutoff angle (Fig. 4) may be useful in discriminating between hanging wall strain caused by a propagating fault tip and strain unrelated to fault propagation. Higher displacement gradients (low relative stretch values) seem to be associated with a propagating fault tip, whereas low displacement gradients (higher relative stretch values) appear to be associated with fault-bend folding.

CONCLUSIONS

As recognized by Williams and Chapman (1983), the processes of fault propagation and displacement are highly dependent on the nature of the ductile strain in the rocks adjacent to the fault. The exact nature of the relationship between these processes, however, may be more complex than previously recognized. Displacement–distance analysis of fault-related fold models reveals the following insights into the relationship between fault propagation, ductile strain, and displacement–distance relationships.

(1) Displacement–distance relationships are highly dependent on the nature of the hanging wall strain. In some cases, different processes can result in similar displacement–distance relationships (i.e. identical relationship between s/p and ε_r in fault-parallel pure shear and fault-propagation fold models), and, in other cases, similar deformation mechanisms can result in different displacement–distance relationships (i.e. bedding-parallel simple shear in both fault-propagation fold and fault-bend fold models).

(2) In general, relative stretch is not related to s/p in any simple way. Displacement–distance relationships for fault-propagation fold models with linear displacement gradients appear to be described accurately by equation (1). However, displacement–distance relationships for fault-bend folds and décollement folds are not. Thus fault propagation histories cannot be uniquely determined from displacement–distance relationships in most cases.

(3) Deformation by simple shear in response to slip on a non-planar fault may yield displacement gradients that are not related to fault propagation. Thus fault tip locations cannot always be predicted by linear extrapolation of displacement–distance trajectories.

(4) Simple shear may result in displacement maxima that are unrelated to fault propagation. Therefore, displacement maxima are not necessarily indicative of fault nucleation points in all cases.

(5) Although calculation of s/p ratios from observed relative stretch magnitudes may not be appropriate, the use of displacement–distance relationships can nonetheless be useful in comparing structures and improving structural interpretations.

Acknowledgements—This study has benefitted from the comments of E. A. Erslev, R. Groshong, P. Hudleston, and R. Price, and reviews by D. M. Fisher, R. Groshong, and M. S. Wilkerson. This project was supported by funding from the National Science Foundation (grant EAR-9304547 to E. A. Erslev), a research assistantship from the Department of Earth Resources and the Hill Memorial Fellowship from the College of Natural Resources at Colorado State University. The author acknowledges Cogniseis Development, M. G. Rowan, R. Kligfield, and P. Weimer for access to GEOSEC™ software.

REFERENCES

Chapman, T. J. and Williams, G. D. (1984) Displacement–distance methods in the analysis of fold–thrust structures and linked-fault systems. *Journal of the Geological Society of London* **141**, 121–128.

Chapple, W. M. and Spang, J. H. (1974) Significance of layer-parallel slip during folding of layered sedimentary rocks. *Geological Society of America Bulletin* **85**, 1523–1534.

Chester, J. S. and Chester, F. M. (1990) Fault-propagation folds above thrusts with constant dip. *Journal of Structural Geology* **12**, 903–910.

Coward, M. P. and Kim, J. H. (1981) Strain within thrust sheets. In *Thrust and Nappe Tectonics*, eds K. R. McClay and N. J. Price, pp. 275–291. The Geological Society of London.

DePaor, D. G. (1987) Stretch in shear zones: implications for section balancing. *Journal of Structural Geology* **9**, 893–895.

Dominic, J. B. and McConnell, D. A. (1994) The influence of structural lithic units in fault-related folds, Seminoe Mountains, Wyoming, U.S.A. *Journal of Structural Geology* **16**, 769–779.

Elliott, D. (1976) The energy balance and deformation mechanisms of thrust sheets. *Philosophical Transactions of the Royal Society of London* **283**, 289–312.

Ellis, M. A. and Dunlap, W. J. (1988) Displacement variation along thrust faults: implications for the development of large faults. *Journal of Structural Geology* **10**, 183–192.
Erslev, E. A. (1991) Trishear fault-propagation folding. *Geology* **19**, 617–620.
Ferrill, D. A. (1988) Use of fault cut-offs and bed travel distance in balanced cross-sections: Discussion 2. *Journal of Structural Geology* **10**, 313–314.
Geiser, P. A. (1988) Mechanisms of thrust propagation: some examples and implications for the analysis of overthrust terranes. *Journal of Structural Geology* **10**, 829–845.
Geiser, J., Geiser, P. A., Kligfield, R., Ratliff, R. and Rowan, M. (1988) New applications of computer-based section construction: Strain analysis, local balancing, and subsurface fault prediction. *Mountain Geologist* **25**, 47–59.
Geiser, P. A. and Engelder, T. (1984) The distribution of layer parallel shortening fabrics in the Appalachian foreland of New York and Pennsylvania: evidence for two non-coaxial phases of the Alleghanian orogeny. In *Tectonics and Geophysics of Memoirs of the Geological Society of America* **158**, 161–175.
Goguel, J. (1962) *Tectonics*. W. H. Freeman and Co. San Fransisco.
Homza, T. X. and Wallace, W. K. (1995) Geometric and kinematic models for detachment folds with fixed and variable detachment depths. *Journal of Structural Geology* **17**, 575–588.
Jamison, W. R. (1987) Geometric analysis of fold development in overthrust terranes. *Journal of Structural Geology* **9**, 207–219.
Kattenhorn, S. A. and McConnell, D. A. (1993) Displacement–distance diagrams applied to the analysis of fault-propagation folds. *Geological Society of America Abstracts with Programs* **26**, 170.
Laubscher, H. P. (1977) Fold development in the Jura. *Tectonophysics* **37**, 337–362.
McConnell, D. A. (1994) Fixed-hinge, basement-involved fault-propagation folds, Wyoming. *Geological Society of America Bulletin* **106**, 1583–1593.
Mitra, S. (1990) Fault-propagation folds: Geometry, kinematic evolution, and hydrocarbon traps. *Bulletin of the American Association of Petroleum Geologists* **74**, 921–945.
Mitra, S. and Namson, J. (1989) Equal-area balancing. *American Journal of Science* **289**, 563–599.
Rich, R. L. (1934) Mechanics of low-angle overthrust faulting as illustrated by Cumberland thrust block, Virginia, Kentucky, and Tennessee. *Bulletin of the American Association of Petroleum Geologists* **18**, 1584–1596.
Rowan, M. G. and Ratliff, R. A. (1988) Use of fault cut-offs and bed travel distance in balanced cross-sections: Discussion 1. *Journal of Structural Geology* **10**, 311–312.
Sanderson, D. J. (1982) Models of strain variation in nappes and thrust sheets: a review. *Tectonophysics* **88**, 201–233.
Suppe, J. (1983) Geometry and kinematics of fault-bend folding. *American Journal of Science* **283**, 648–721.
Suppe, J. and Medwedeff, D. A. (1984) Fault-propagation folding . *Geological Society of America Abstracts with Programs* **16**, 670.
Suppe, J. and Medwedeff, D. A. (1990) Geometry and kinematics of fault-propagation folding. *Eclogae Geologicae Helvetiae* **83**, 409–454.
Williams, G. and Chapman, T. (1983) Strains developed in the hanging-walls of thrusts due to their slip/propagation rate: a dislocation model. *Journal of Structural Geology* **5**, 563–571.

APPENDIX

s/p ratio in fault-propagation fold models

Fault-propagation fold models (Suppe and Medwedeff, 1990) predict a quantitative relationship between the *s/p* ratio and relative stretch.

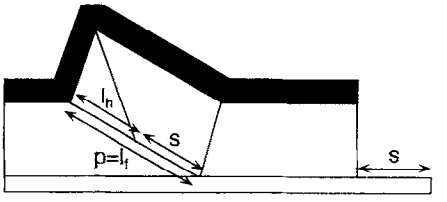

Fig. A1. Fault-propagation fold model showing the parameters used in derivation of the relationship between relative stretch and *s/p* for fault-propagation folds.

Because the bed length is constant along the lower flat,

$$s + l_h = l_f \tag{A1}$$

(Fig. A1). Because the ramp length represents the distance the fault has propagated,

$$l_f = p. \tag{A2}$$

Dividing equation (A1) by l_f,

$$\frac{s + l_h}{l_f} = 1. \tag{A3}$$

Substituting equation (A2) into equation (A3),

$$\frac{s}{p} + \frac{l_h}{l_f} = 1. \tag{A4}$$

Substituting equation (2) into equation (A4),

$$\varepsilon_r = 1 - \frac{s}{p}. \tag{A5}$$

Notice that this relationship is identical to that derived by Williams and Chapman (1983) for the case of fault-parallel pure shear in equation (1). Thus despite the fact the the type of shear is completely different in the Williams and Chapman (1983) pure shear model and the fault-propagation fold model (bedding-parallel simple shear), the relationships between *s/p* ratio and relative stretch are identical.